# Supplementary Information

## Decisive Roles of Interfacial Water Orientation and Hydrogen Bonds in the Dramatic Activity Gap of Metal-Nitrogen-Carbon Catalysts for ORR in Alkaline and Acid

Peng Li‡, Yuzhou Jiao‡, Yana Men, Shengli Chen*

College of Chemistry and Molecular Sciences, Wuhan University, Wuhan 430072, China

‡These authors contributed equally.

*Corresponding Author: slchen@whu.edu.cn

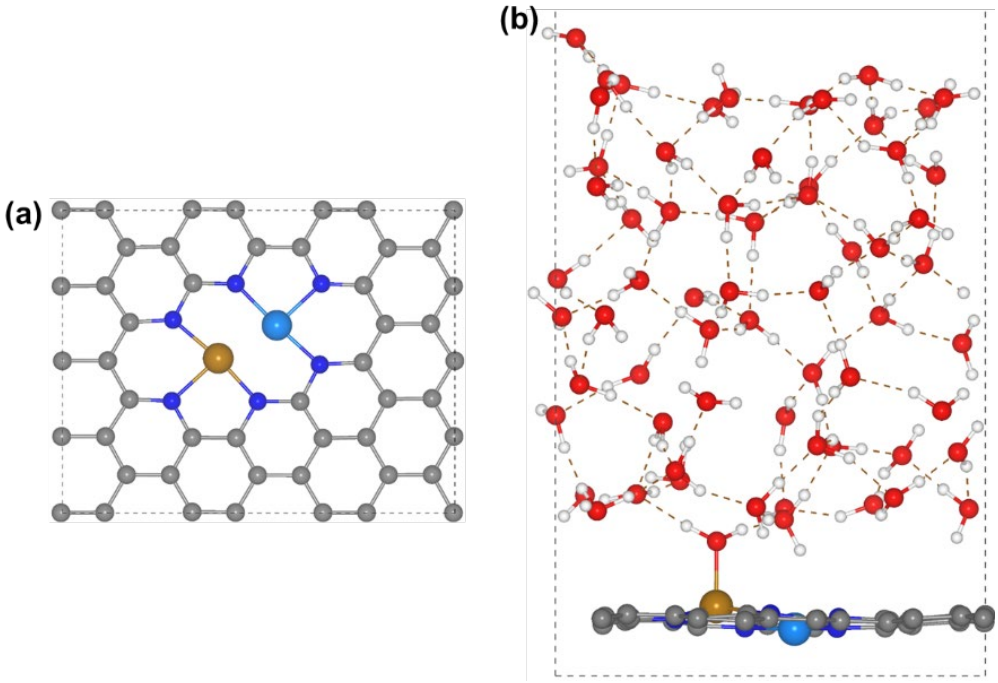


**Supplementary Figure 1.** (a) Structure model of FeCo-$N_6$-C catalyst. (b) Representative snapshot of FeCo-$N_6$-C/water interface at the potential of zero charge (PZC). The Fe, Co, N, C, O and H atoms are colored with brown, sky blue, blue, gray, red and white, respectively (similarly hereinafter). The brown dashed lines represent the hydrogen bonds.

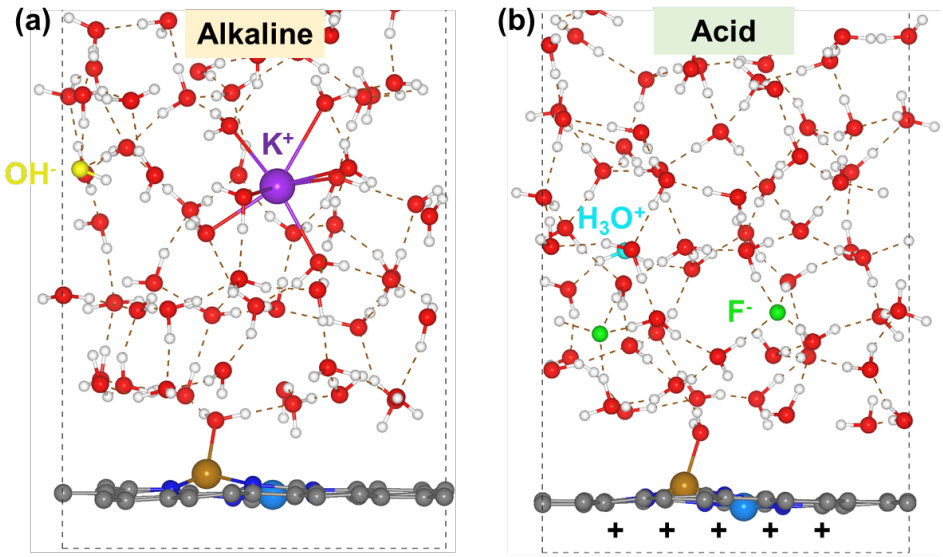


**Supplementary Figure 2.** Representative snapshots of the interfacial structures at ORR potentials on the bare FeCo-$N_6$-C electrode surface for (a) alkaline system and (b) acid system. The $K^+$, $OH^-$, $H_3O^+$ and $F^-$ are colored with purple, yellow, green and cyan, respectively (similarly hereinafter). The brown dashed lines represent the hydrogen bonds.

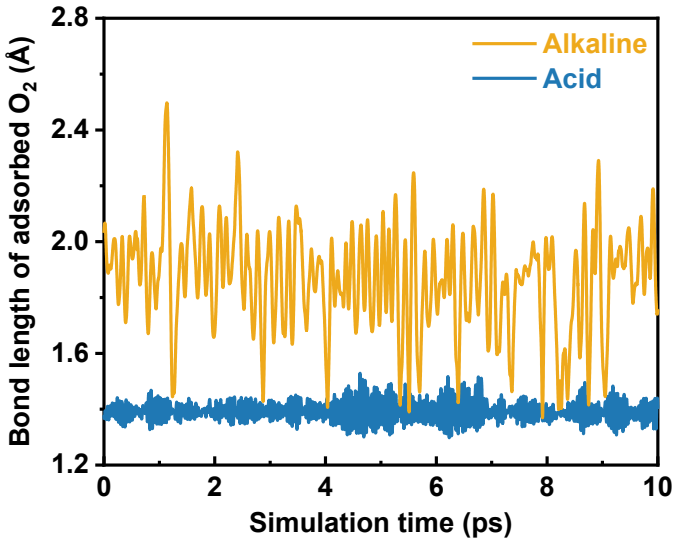


**Supplementary Figure 3.** Comparison of the bond lengths of adsorbed $O_2$ at alkaline and acid interfaces among the whole 10 ps AIMD simulations.

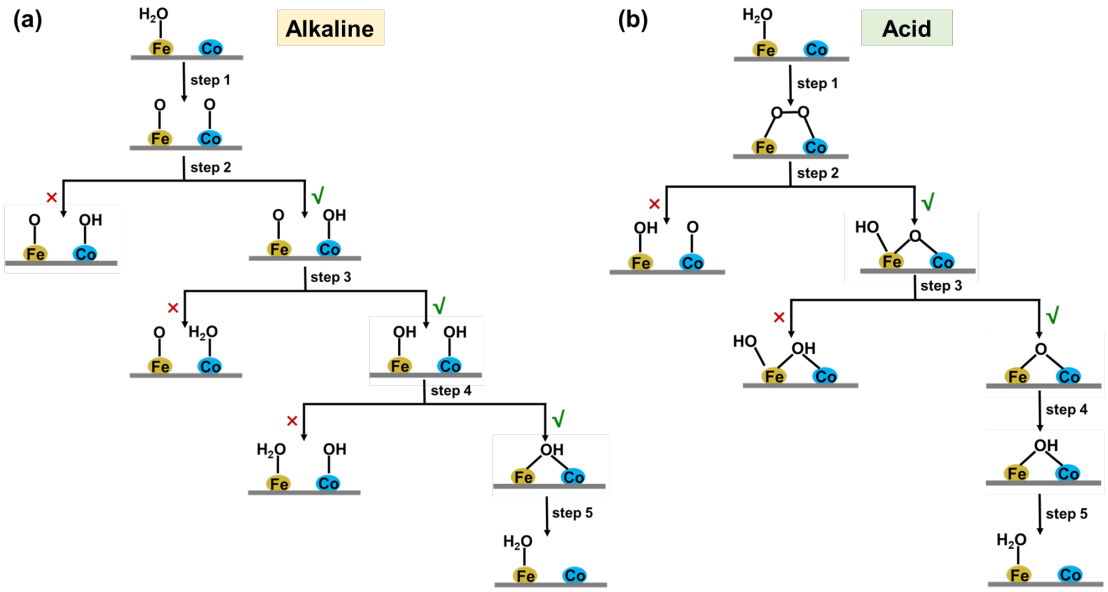


**Supplementary Figure 4.** Schematic diagrams of the determination processes of ORR mechanisms under (a) alkaline and (b) acid condition. In each step, all possible reaction products have been simulated through AIMD to obtain the statistical average of total energy for comparison. The green ticks represent the selected final products, and the red crosses represent the excluded product states with higher energy.

(a)

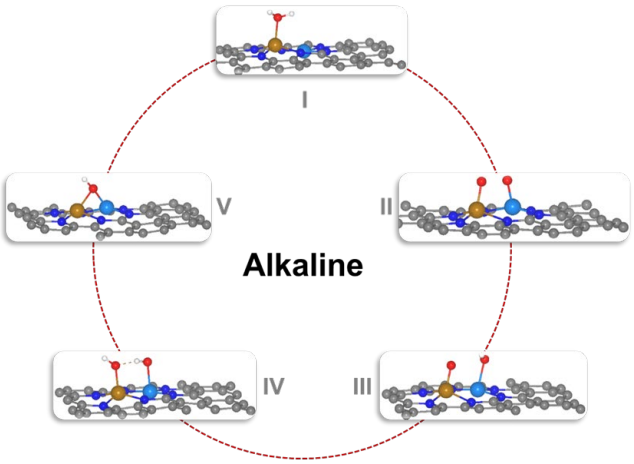


(b)

**Alkaline ORR mechanism**

| | | |
|---|---|---|
| *(Co)-*$H_2O$(Fe) + $O_2$ → *O(Co)-*O(Fe) | R-1 | Chemisorption |
| *O(Co)-*O(Fe) + $H_2O$ + $e^-$ → *OH(Co)-*O(Fe) + $OH^-$ | R-2 | PCET |
| *OH(Co)-*O(Fe) + $H_2O$ + $e^-$ → *OH(Co)-*OH(Fe) + $OH^-$ | R-3 | PCET |
| *OH(Co)-*OH(Fe) + $H_2O$ + $e^-$ → *(Co)-*OH(Fe) + $H_2O$ + $OH^-$ | R-4 | PCET |
| *(Co)-*OH(Fe) + $H_2O$ + $e^-$ → *(Co)-*$H_2O$(Fe) + $OH^-$ | R-5 | PCET |

**Supplementary Figure 5.** (a) Close-up of the ORR process at alkaline interface. The electrolyte environment is not displayed. (b) The corresponding elementary reaction equations along the determined ORR pathway at alkaline interface. The $H_2O$ marked by red color represent the interfacial water molecules which serve as the proton donors and provide H atoms to surface oxygenated intermediates, while the $H_2O$ marked by green color mean the reaction products of ORR.

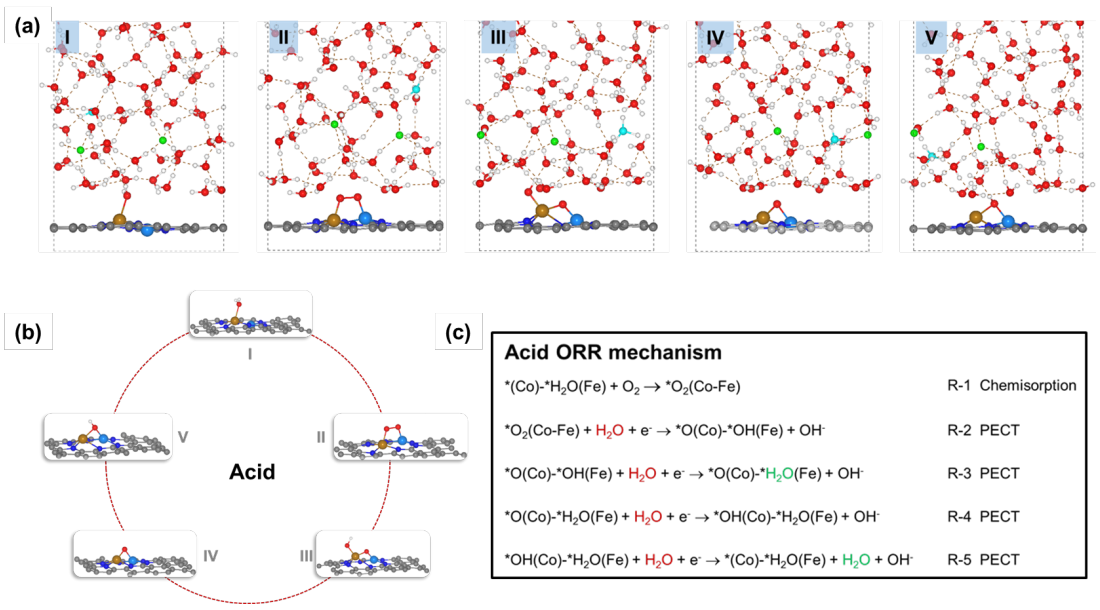


**Supplementary Figure 6.** (a) Representative snapshots of the interfacial structures along the ORR process in acid media. (b) Close-up of the ORR process at acid interface. The electrolyte environment is not displayed. (c) The corresponding elementary reaction equations along the determined ORR pathway at acid interface. The $H_2O$ marked by red color represent the interfacial water molecules which serve as the proton donors and provide H atoms to surface oxygenated intermediates, while the $H_2O$ marked by green color mean the reaction products of ORR. The generated $OH^-$ species will be naturally neutralized by hydronium ions in bulk solution, which is not displayed here.

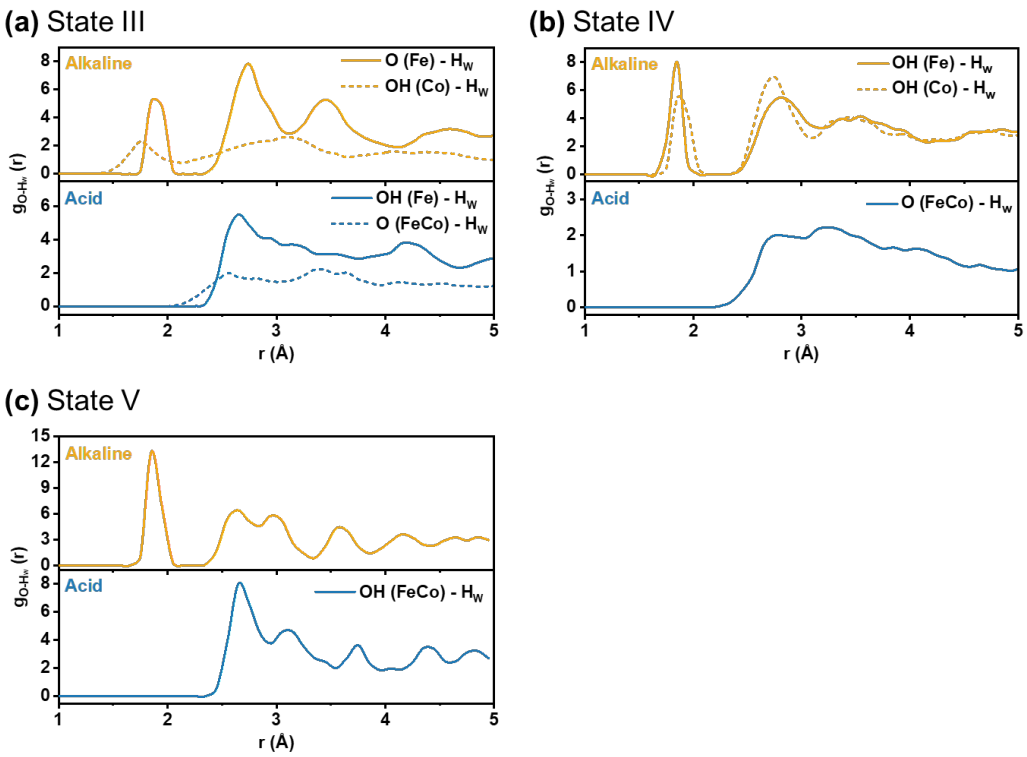


**Supplementary Figure 7.** Radial distribution functions between the O atoms of surface oxygenated intermediates in various reaction intermediate states and the H atoms of interfacial water at alkaline and acid interfaces. Figures a-c correspond to the state III-V shown in Fig. 3c and Supplementary Fig. 6a.

At each reaction intermediate state of alkaline ORR, it is apparent that the radial distribution functions exhibit sharp peaks around 1.85 Å, which indicates the formation of hydrogen bonds between the O atoms of various oxygenated intermediates with the H atoms of interfacial water in alkaline media. By contrast, the radial distribution functions for acid interface do not exhibit peaks within ~2.35 Å, indicating the missing of such hydrogen bonds.

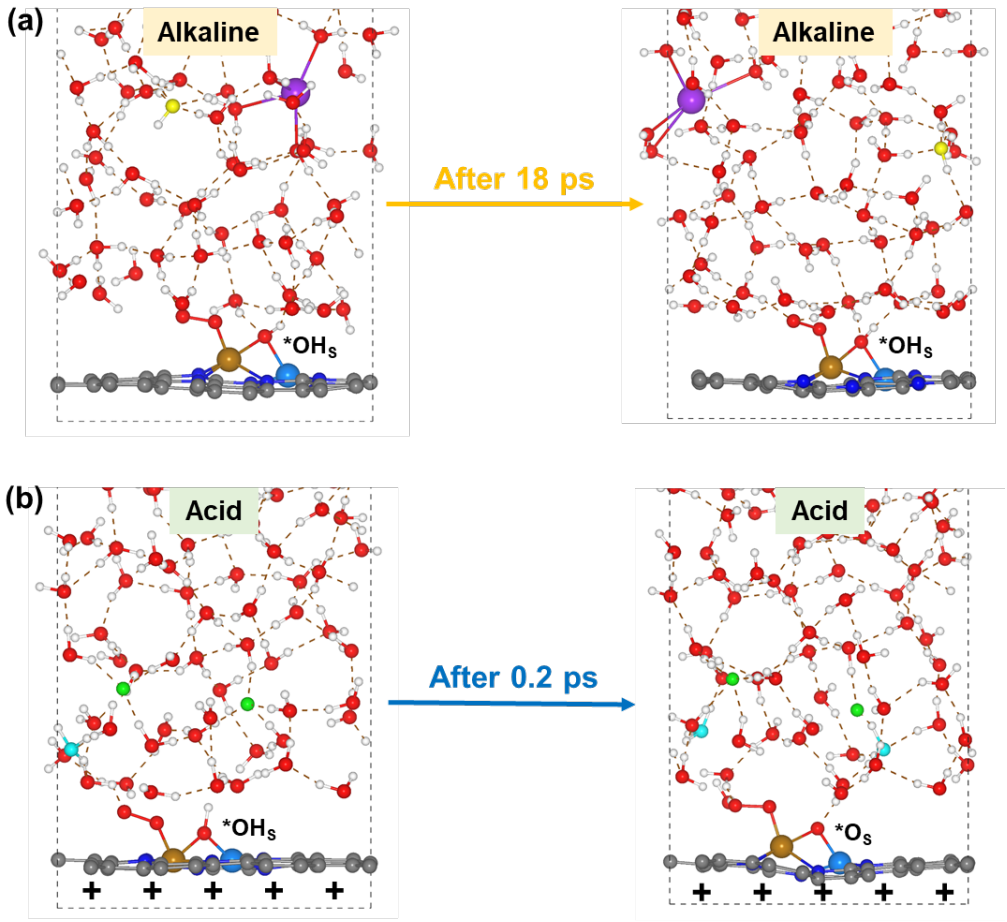


**Supplementary Figure 8.** The interface structures in (a) alkaline and (b) acid medias before and after AIMD simulations.

It is known that the oxygenated species, *OH or *O, often occupy the surface sites and act as the spectators in ORR process. For DAC catalysts, these strong adsorption of oxygenated intermediates on the bridge site of two metal atoms (see State V in Fig. 3a and States III-V in Fig. 3b for examples) is very likely to result in the existence of oxygenated spectators. Such scenario has been considered in this work.

To determine what exactly the surface oxygenated spectators are in alkaline and acid medias under experiment ORR potentials, the *OH oxygenated species on the Fe-Co bridge sites are evaluated, as shown in the left panels of Supplementary Fig. 8a,b. At alkaline interface, the *OH occupying the Fe-Co bridge site remains stable throughout the 18 ps AIMD simulation (Supplementary Fig. 8a), which implies that the oxygenated spectator should be *OH (termed as $*OH_S$). While at acid interface, the *OH occupying the Fe-Co bridge site is oxidized

spontaneously and turns into a *O species and a $H_3O^+$ cation after merely 0.2 ps AIMD simulation (Supplementary Fig. 8b), which indicates that the oxygenated spectator should be *O (termed as $*O_S$). This difference in oxygenated spectator between alkaline and acid systems can be attributed to the difference in surface charge densities of FeCo-$N_6$-C electrodes. Clearly, the positively charged FeCo-$N_6$-C electrode can induce the transition of *OH to *O.

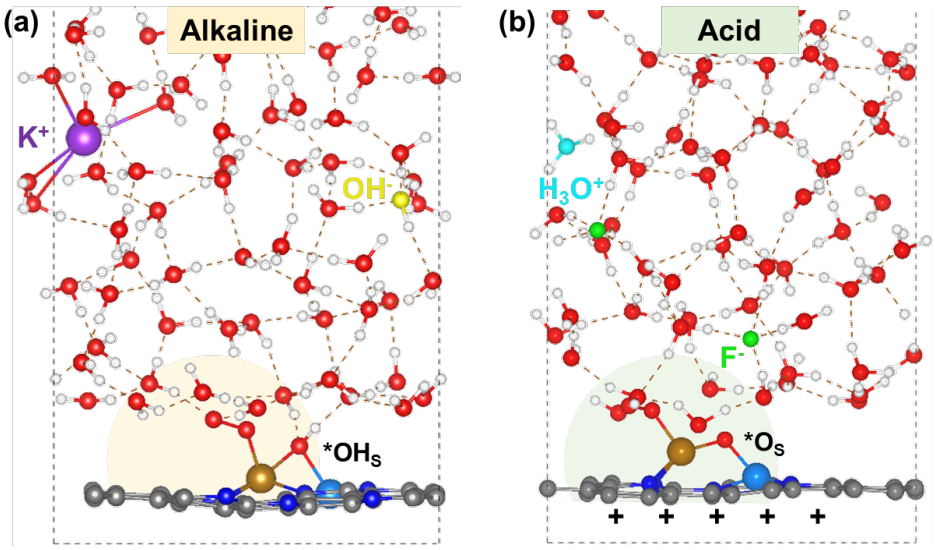


**Supplementary Figure 9.** Representative snapshots of the interfacial structures at ORR potentials in (a) alkaline and (b) acid electrolytes with the existence of adsorbed $O_2$ molecules and oxygenated spectators on FeCo-$N_6$-C.

In both alkaline and acid medias, the $O_2$ molecules are adsorbed on Fe sites with end-on configuration, due to the occupation of Fe-Co bridge sites by the oxygenated spectators (*$OH_S$ in alkaline and *$O_S$ in acid) and the stronger affinity of Fe element for oxygenated species. At this time, there are still one $K^+$ cation and one $OH^-$ anion being introduced into the water film to simulate the alkaline environment, and one $H_3O^+$ cation and two $F^-$ anions being introduced into the water film to simulate the acid environment. The electrode potentials are calculated as ~1.0 V and ~0.8 V for alkaline and acid systems, respectively, which also correspond to the experimental ORR potentials.

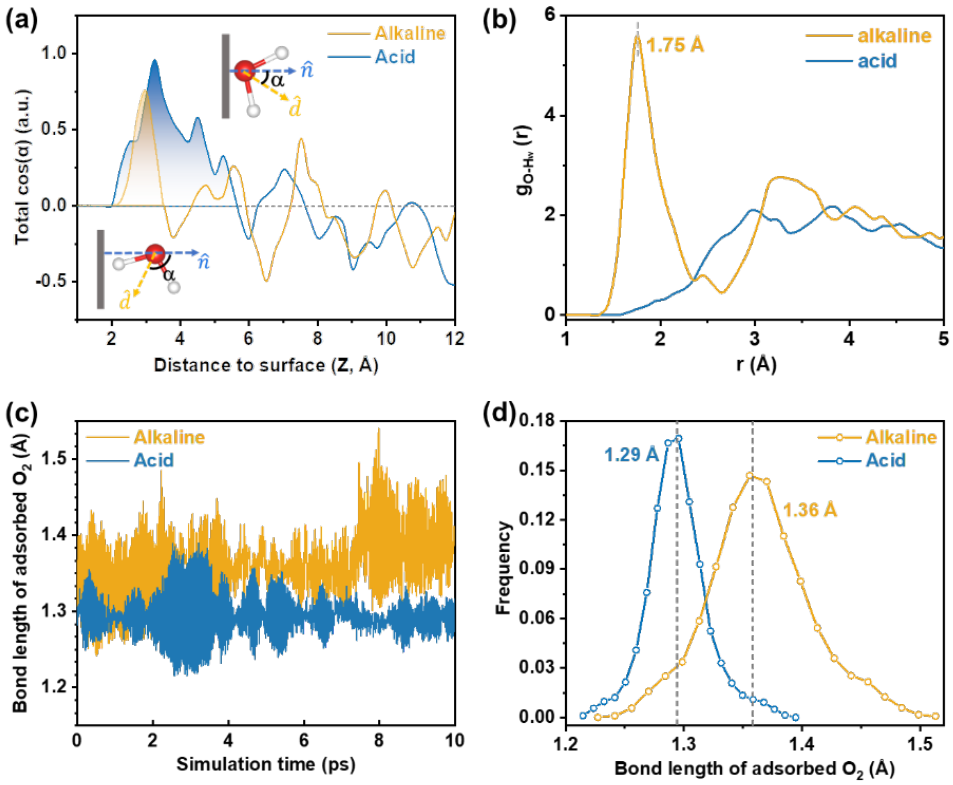


**Supplementary Figure 10.** (a) Distribution profiles of water dipole orientations along the surface normal direction at acid and alkaline interfaces. The insets show that α is defined as the angle between the vector of water dipole ($\hat{d}$) and the surface normal ($\hat{n}$). (b) Radial distribution functions between the O atom of adsorbed $O_2$ molecule that points to the solution and the H atoms of interfacial water. (c) The extraction of O-O bond length of the adsorbed $O_2$ molecule during the 10 ps AIMD product simulations for alkaline and acid systems. (d) Statistical distributions of the O-O bond length of adsorbed $O_2$ molecule at acid and alkaline interfaces.

The distribution of total cosα displays a series of peaks with much higher amplitudes within ~5.6 Å at acid interface while only a fairly weak and narrow peak within ~3.5 Å at alkaline interface (Supplementary Fig. 10a). This implies that despite the presence of *$OH_S$ and *$O_S$ oxygenated spectators, the interfacial water molecules are still orientated orderly in the form of O-down configuration due to the positively charged electrode surface in acid media, while disorderly in alkaline media. Correspondingly, the O atom of end-on adsorbed $O_2$ that points to the solution can form the hydrogen bonds with the H atoms of interfacial water in alkaline media

(Supplementary Fig. 10b). Furthermore, it can be seen that the O-O bond length of adsorbed $O_2$ molecule at alkaline interface is obviously larger than that at acid interface (1.36 Å vs 1.29 Å), due to the assistance of hydrogen bonds formed with interfacial water. Notably, compared with the O-O bond length (1.90 Å) at the alkaline interface without oxygenated spectators (Fig. 1a and 2d), the adsorbed $O_2$ molecule in the end-on configuration at the alkaline interface with the existence of $*OH_S$ spectator does not dissociate.

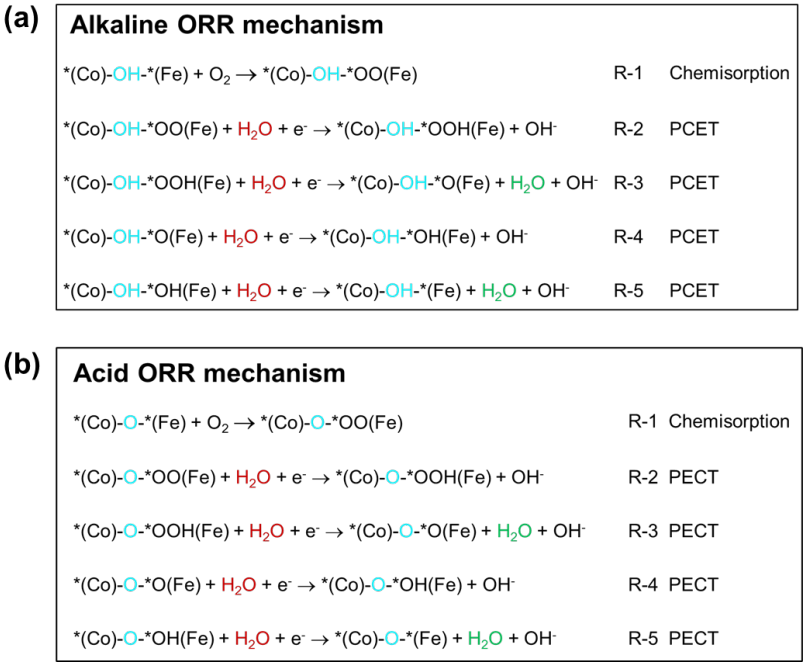


**Supplementary Figure 11.** The determined ORR mechanism at (a) alkaline and (b) acid interface when the oxygenate spectator (*$OH_S$, marked by cyan color) is considered. The $H_2O$ marked by red color represent the water molecules which locate in the solution and provide proton to surface oxygenated intermediates, while the $H_2O$ marked by green color mean the reaction products.

It can be noted that due to the existence of oxygenated spectators, the Co atom with relatively weak oxygenophilicity has been poisoned and thereby the synergistic effect between adjacent metal active sites is broken. Therefore, at both alkaline and acid interfaces with the existence of spectators, the adsorbed $O_2$ molecules in the end-on configurations do not dissociate (Supplementary Fig. 9 and 10d), resulting in the formation of the *OOH intermediates. At this time, it can be realized that the FeCo-$N_6$-C double atom catalyst is similar to the Fe-$N_3O$-C single atom catalyst to a certain extent.

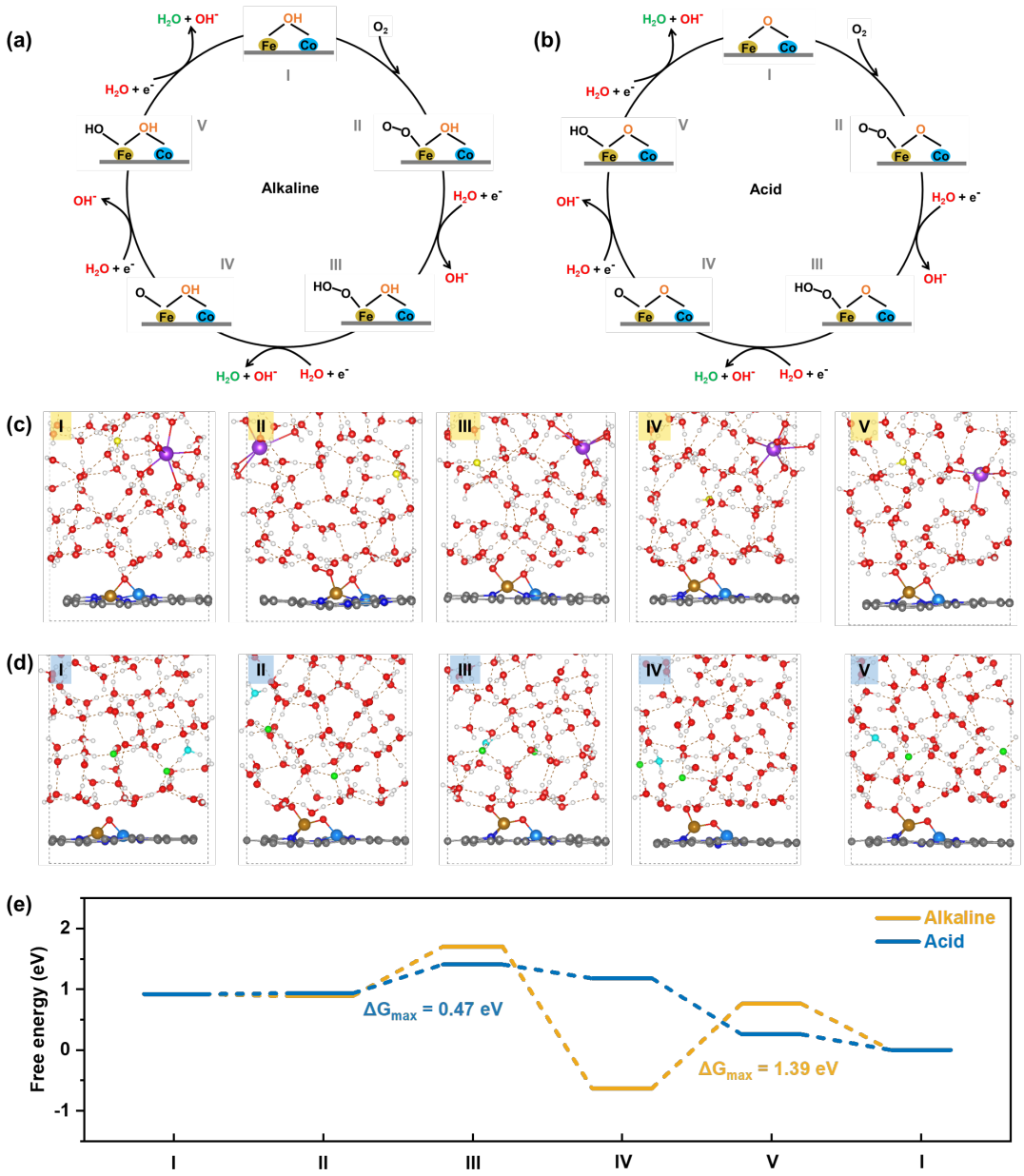


**Supplementary Figure 12.** (a,b) Schematic diagrams of ORR processes in (a) alkaline and (b) acid medias when the oxygenated spectators (marked by orange color) are considered. The $H_2O$ marked by red color represent the water molecules which locate in the solution and provide proton to surface oxygenated intermediates, while the $H_2O$ marked by green color mean the reaction products. (c,d) Representative snapshots of the interfacial structures along the ORR processes in (c) alkaline and (d) acid medias. (e) Free energy diagrams for ORR at alkaline and acid interfaces for U = 1.0 V vs RHE.

In the presence of oxygenated spectators, the third PCET step (IV→V in Supplementary Fig. 12a) is the PDS of alkaline ORR; while for acid ORR, the PDS is the first PCET step (II→III in

Supplementary Fig. 12b). Notably, the free energy change of PDS at acid interface is still much smaller than that at alkaline interface (0.47 eV vs 1.39 eV), contradicting the experimental truth that the ORR activity in alkaline is superior to that in acid.

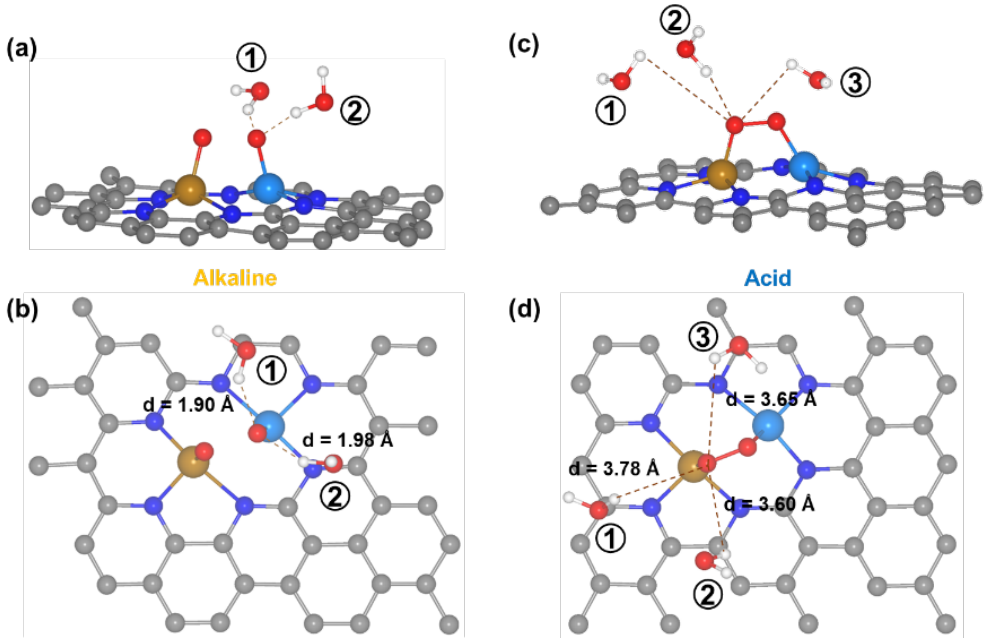


**Supplementary Figure 13.** (a,b) Close-up of two interfacial water molecules that form hydrogen bonds (brown dashed lines) with the O atom on Co site for alkaline system. (a) side view; (b) top view. The indexes of these two water molecules and the corresponding length of hydrogen bonds are shown. (c,d) Close-up of three interfacial water molecules closest to the O atom on Fe site for acid system. (c) side view; (d) top view. The indexes of these three water molecules and the corresponding distances between the H atom of water and O atom on Fe site are shown.

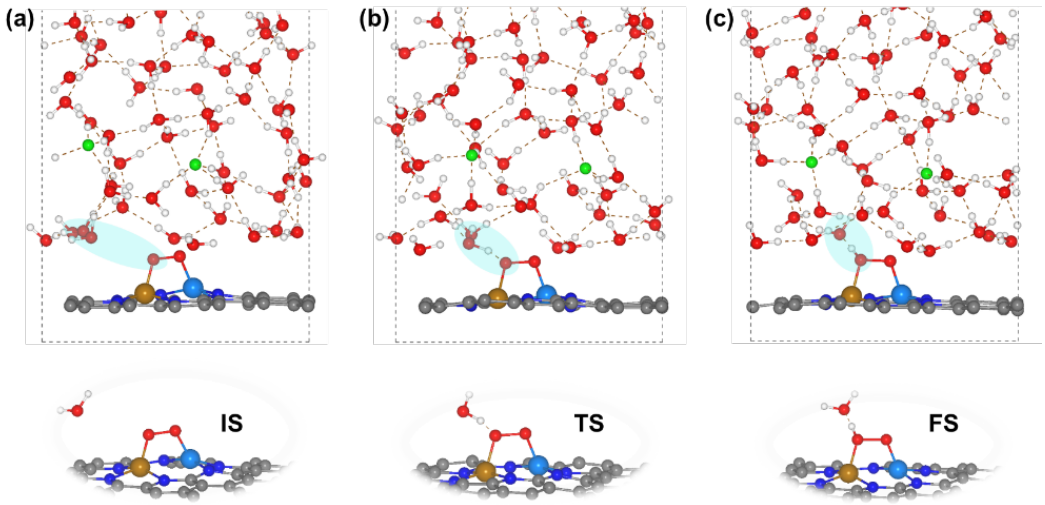


**Supplementary Figure 14.** (a-c) The interface structures (upper panel) and corresponding close-up (lower panel) of the initial state (IS), transition state (TS) and final state (FS) in one typical slow-growth simulation for the first PCET reaction of acid ORR.

At acid interface, in the process from IS to TS, the reactive water molecule first gradually approaches the O atom on Fe site with maintaining the O-down configuration, and then its orientation is flipped to the 'one-H-down' configuration in order to provide the H atom to the O atom of adsorbed $O_2$ molecule. Due to the strong electrostatic interaction to interfacial water molecule exerted by the positively charged FeCo-$N_6$-C electrode, the flip of water dipole orientation contributes to a fairly high barrier. The following process from TS to IS corresponds to the bond formation between the O atom of $O_2$ on Fe site and the H atom of reactive water molecule, and meanwhile the generated $OH^-$ anion turns into water molecule by receiving a H atom from another water molecule that locates further away from the electrode.

**Supplementary Note 1: constant potential correction.**

In the actual electrocatalytic reaction process, the electrode potential always keeps constant. However, in the AIMD simulation, it is the charge of the system that keeps constant; while the work function and electrode potential changes moment by moment along the reaction process. Thus, we need to correct the calculated energy change to conform the constant-potential condition.

For a constant-charge simulation from state 1 to state 2, we can calculate the corresponding total energies $E_1(\Phi_1)$ and $E_2(\Phi_2)$, work functions $\Phi_1$ and $\Phi_2$, as well as the number of excess electrons in the slabs $q_1$ and $q_2$ using Bader analysis. According to the works of Chan and Nørskov,[1,2] we can use these data to calculate the corresponding energy change between the two states at a certain work function. For example, we can calculate the energy change at constant potential $\Phi_1$ using the following equation:

$$E_2(\Phi_1) - E_1(\Phi_1) = E_2(\Phi_2) - E_1(\Phi_1) + \frac{(q_2 - q_1)(\Phi_2 - \Phi_1)}{2} \qquad (1)$$

**Supplementary Note 2: slow-growth approach**

The free energy profile along a collective variable (CV, $\xi$) can be scanned by an approximate slow-growth approach.[3] In this method, the value of $\xi$ is linearly changed from the value characteristic for state 1 to that for state 2 with a velocity of transformation $\dot{\xi}$. The resulting work needed to perform a transformation 1→2 can be computed as:

$$w_{1\to2}^{irrev} = \int_{\xi_1}^{\xi_2} \left(\frac{\partial F(q)}{\partial \xi}\right) \cdot \dot{\xi} dt \qquad (2)$$

where $F(q)$ is the free energy at general coordinate $q$ which is evolving with time $t$, $\frac{\partial F}{\partial \xi}$ is calculated along the track of a constrained MD through the SHAKE algorithm.

In the limit of infinitesimally small $\dot{\xi}$, the work $w_{1\to2}^{irrev}$ corresponds to the free-energy difference between state 1 and state 2. In the general case, $w_{1\to2}^{irrev}$ is the irreversible work related to the free energy via Jarzynski's identity:

$$exp\left\{-\frac{\Delta F_{1\to2}}{k_B T}\right\} = \langle exp\left\{-\frac{w_{1\to2}^{irrev}}{k_B T}\right\}\rangle \qquad (3)$$

where $\langle \ldots \rangle$ stand for the statistical average of the term enclosed in angular parentheses.

**Supplementary Note 3: The free energy diagram calculation**

For the chemisorption step of $O_2$ molecule, the free energy change is calculated by the following equation:

$$\Delta G = \left(\langle E_{*O_2}\rangle + ZPE_{*O_2} - TS_{*O_2}\right) - \langle E_*\rangle - \left(E_{O_2} + ZPE_{O_2} - TS_{O_2}\right) - \Delta E_{corr} \quad (4)$$

where $\langle E_{*O_2}\rangle$ and $\langle E_*\rangle$ are the statistically averaged internal energies of interface systems before and after $O_2$ adsorption; $ZPE$ and $TS$ are the corresponding zero-point energy and vibrational entropy of reaction intermediate; $E_{H_2}$ is the internal energy of $H_2$(g).

For each PCET reaction in the alkaline and acid ORR, the free energy change is calculated by the following equation:

$$\Delta G = (\langle E_{*B}\rangle + ZPE_{*B} - TS_{*B}) - (\langle E_{*A}\rangle + ZPE_{*A} - TS_{*A}) - \frac{1}{2}\left(E_{H_2} + ZPE_{H_2} - TS_{H_2}\right) + e(U - U_{cal}) \quad - \Delta E_{corr} \quad (5)$$

where $\langle E_{*A}\rangle$ and $\langle E_{*B}\rangle$ are the statistically averaged internal energies of interface systems before and after PCET reaction (A and B represent the surface reaction intermediates); $ZPE$ and $TS$ are the corresponding zero-point energy and vibrational entropy of reaction intermediate; $E_{H_2}$ is the internal energy of $H_2$(g). If the PCET reaction generates water molecule product, the $\Delta G$ should also add the term $E_{H_2O} + ZPE_{H_2O} - TS_{H_2O}$. All values of ***ZPE*** and ***TS*** are from previous reports.[4,5] Because the work function changes after reaction, the constant potential correction has been performed, and the correction term $\Delta E_{corr}$ equals to $\frac{(q_2 - q_1)(\Phi_2 - \Phi_1)}{2}$. In addition, in the construction of the free energy diagrams for ORR, the electrode potentials ($U$) for alkaline and acid systems have been set as the same value (1.0 V vs RHE), which is convenient for the comparison of the reaction thermodynamics. Therefore, the $\Delta G$ of an PCET step has been adjusted by the term $e(U - U_{cal})$, in which the $U_{cal}$ is the calculated electrode potential of the AIMD simulated interfaces shown in Fig. 1 and Supplementary Fig. 9.

## Supplementary References


1. Chan, K. & Nørskov, J. K. Electrochemical barriers made simple. *J. Phys. Chem. Lett.* **6,** 2663-2668 (2015).
2. Chan, K. & Nørskov, J. K. Potential dependence of electrochemical barriers from ab initio calculations. *J. Phys. Chem. Lett.* **7,** 1686-1690 (2016).
3. Woo, T. K., Margl, P. M., Blöchl, P. E. & Ziegler, T. A combined Car−Parrinello QM/MM implementation for ab initio molecular dynamics simulations of extended systems: application to transition metal catalysis. *J. Phys. Chem. B* **101,** 7877-7880 (1997).
4. Nørskov, J. K. et al. Origin of the overpotential for oxygen reduction at a fuel-cell cathode. *J. Phys. Chem. B* **108,** 17886-17892 (2004).
5. Rossmeisl, J., Logadottir, A. & Nørskov, J. K. Electrolysis of water on (oxidized) metal surfaces. *Chem. Phys*. **319,** 178-184 (2005).